Food and Bioprocess Technology (2022) 15:1284–1298
https://doi.org/10.1007/s11947-022-02815-2

ORIGINAL RESEARCH

Active Composite Packaging Reinforced with Nisin-Loaded Nano-Vesicles for Extended Shelf Life of Chicken Breast Filets and Cheese Slices

Taskeen Niaz[1,2] · Saima Shabbir[3] · Tayyaba Noor[4] · Muhammad Imran[1]

Received: 29 November 2021 / Accepted: 14 April 2022 / Published online: 23 April 2022

Abstract

To meet the demands for more effective and ecofriendly food packaging strategies, the potential of nisin-loaded rhamnolipid functionalized nanofillers (rhamnosomes) has been explored after embedding in hydroxypropyl-methylcellulose (HPMC) and κ-carrageenan (κ-CR)-based packaging films. It was observed that intrinsically active rhamnosomes based nanofillers greatly improved the mechanical and optical properties of nano-active packaging (NAP) films. Incorporation of rhamnosomes resulted in higher tensile strength (5.16 ± 0.06 MPa), Young's modulus (2777 ± 0.77 MPa), and elongation (2.58 ± 0.03%) for NAP than active packaging containing free nisin (2.96 ± 0.03 MPa, 1107 ± 0.67 MPa, 1.48 ± 0.06%, respectively). NAP demonstrated a homogenous distribution of nanofillers in the biopolymer matrix as elucidated by scanning electron microscopy (SEM). Thermogravimetric analysis (TGA) confirmed that NAP prepared with nisin-loaded rhamnosomes was thermally stable even above 200 °C. Differential scanning calorimetry (DSC) analyses revealed that addition of nisin in nanofillers resulted in a slight increase in Tg (108.40 °C), indicating thermal stability of NAP. Fourier transform infrared spectroscopy (FTIR) revealed slight shift in all characteristic bands of nano-active packaging, which indicated the embedding of rhamnosomes inside the polymer network without any chemical interaction. Finally, when tested on chicken breast filets and cheese slices under refrigerated storage conditions, NAP demonstrated broad-spectrum antimicrobial activity (up to 4.5 log unit reduction) and inhibited the growth of *Listeria monocytogenes*, *Staphylococcus aureus*, *Pseudomonas aeruginosa*, and *Escherichia coli*. These results suggest that HPMC and κ-CR-based NAP containing functionalized nanofillers can serve as an innovative packaging material for the food industry to improve the safety, quality, and shelf-life of dairy and meat products.

Keywords Nano-active packaging · κ-carrageenan · HPMC · Rhamnolipids · Functionalized liposome · Nisin

Introduction

During the current COVID-19 pandemic, increased consumer demand for hygienic, safe, and good quality food products with improved shelf life has intensified the use of packaging materials for food safety. Majority of current food packaging materials are plastic-based and non-biodegradable, which increase the risk of plastic waste and its negative effect on the economy (high oil prices) and environment (solid waste). In this scenario, European Union announced post-pandemic policy goals (e.g., Green Deal, Post-pandemic Action Plan for a Circular Economy) for the food packaging industry, which aims to reduce 70% of the plastic use by 2030 (Gottardo et al., 2021). This aim would be realized by promoting ecofriendly and bio-based packaging materials with improved shelf life and safety. It is estimated that by 2026, the global market share of bio-based packaging material will increase up to 50% (Kochańska et al., 2021).

To meet the demands for more effective and alternative food packaging strategies, numerous biodegradable (polysaccharides, proteins, and lipids) polymers (Aydogdu et al., 2019; Mihalca et al., 2021; Mohamed et al., 2020) have been exploited. Ideal packaging material should not only

✉ Muhammad Imran
m.imran@comsats.edu.pk

1 Department of Biosciences, Faculty of Sciences, COMSATS University Islamabad, Park Road, Islamabad, Pakistan

2 Pakistan Institute of Rehabilitation Sciences (PIRS), ISRA University Islamabad Campus, Islamabad, Pakistan

3 Department of Materials Science and Engineering, Institute of Space Technology, Islamabad 44000, Pakistan

4 School of Chemical and Materials Engineering (SCME), National University of Sciences and Technology (NUST), Islamabad, Pakistan

maintain the shelf life of the food products but also protect food from contaminants and ensure its delivery to consumers in a nutritious form without compromising environmental safety. For this purpose, kappa (κ) carrageenan is an attractive candidate. It consists of repeating units of alternating α-(1–3)-d-galactose and β-(1- 4)-3, 6-anhydro-d-galactose (Souza et al., 2018). Kappa (κ) carrageenan is a natural sulfated polysaccharide extracted from seaweed and can form a hard and firm hydrogel (Zhong et al., 2020). However, the coating derived from the hydrogel is too brittle with insufficient mechanical strength, inadequate thermal stability, and low water vapor barrier properties (Sedayu et al., 2020). Blending with different biopolymers to form composite coatings and the addition of various fillers are some of the common approaches to improve the low tensile strength and brittle properties of biopolymeric films (Malik & Mitra, 2021). Hydroxypropyl methylcellulose (HPMC) can prove to be good candidate for the fabrication of polymeric composite coatings with kappa (κ) carrageenan. HPMC is a potential biopolymer that is widely used in the food packaging industry to form composite coatings with other biopolymers, e.g., polylactic acid (PLA) and hydroxypropyl methylcellulose (HPMC) (Bodbodak et al., 2021), chitosan-HPMC (Bigi et al., 2021), and sodium alginate-HPMC-based composite packaging films (Amjadi et al., 2020).

Active composite coatings are usually obtained by incorporating natural or synthetic antimicrobial agents in food coatings (Sahraee et al., 2017; Samsalee & Sothornvit, 2020). These agents are released slowly into the food to prevent microbial growth. One such antimicrobial agent is nisin, which is the only bacteriocins generally recognized as safe (GRAS) by the Food and Drug Administration (FDA), allowing its use for surface treatment of meat and dairy products (Food and Drug Administration, 2011). However, nisin exhibits antimicrobial activity only against Gram-positive bacteria, i.e., *Listeria monocytogenes* (Pérez et al., 2021). Secondly, the direct addition of free form of bacteriocins, e.g., nisin in these food coatings also faces certain limitations, e.g., immediate inhibition of spoilage microorganisms but the survivor population continues to grow after the depletion of added antimicrobials. This depletion is mainly due to complex interactions with the food matrix or by the natural degradation of antimicrobial peptides with time, causing loss of shelf-life (Becerril et al., 2020). Secondly, due to the high diffusion coefficient and low molecular weight of biopolymeric packaging materials, the release rate of most active compounds is potentially rapid, which reduces the prolonged activity of active coatings during the shelf life of food products (Almasi et al., 2020). These limitations can be overcome by reinforcing the coatings with nano-scale structures or fillers to form nanocomposites coatings. These coatings could not only improve the physical, mechanical, and barrier properties of the packaging materials but also protect the active agent from early degradation and prolong the shelf life of food products by providing sustained release of active agents over longer period (Kamkar et al., 2021; Rehman et al., 2020).

From the last few decades, food industry is utilizing phospholipids-based nanocarriers, i.e., liposomes as nanofillers in the nanocomposite packaging materials to enhance food safety (Aziz & Almasi, 2018; Nazir & Azad, 2019). Despite the above-mentioned benefits of nanocomposite packaging (NCP), some associated challenges such as less stability and sensitivity of nanoliposomes (NLs) towards various processing conditions of packaging materials (for instance temperature) and the recently exhibited resistance against nisin by foodborne pathogens restrict their application in the food industry (Tan et al., 2021). These challenges can be overcome by the development of nanomaterials having intrinsic antimicrobial activity. Rhamnolipid (RL) is a broad-spectrum antimicrobial bio-surfactant with unique physiochemical properties. Functionalization of liposomes with RLs could not only improve the thermal and physical stability of NLs but can also induce intrinsic antimicrobial capacity in NLs against various food spoilage pathogens. Recently, the antimicrobial potential of various inorganic nanofillers (with intrinsic antimicrobial activity) in packaging films has been explored against foodborne pathogens (Amjadi et al., 2019; de Souza et al., 2021; Malik & Mitra, 2021; Ortiz-Duarte et al., 2021; Priyadarshi & Negi, 2017). Similarly, κ-carrageenan (κ-CR) and hydroxypropyl methylcellulose (HPMC) blend-based pH-sensitive intelligent packaging films have been developed recently to evaluate the quality of meat-based products (Chi et al., 2020; Sun et al., 2019). However, the antimicrobial potential of biosurfactant functionalized nanofillers and their synergistic activity with the active agent (nisin) in κ-CR-HPMC-based NCP to extend the shelf life of meat and dairy products has not been explored yet.

The main objective of the present study will be to explore the impact of rhamnolipid functionalized nanofillers on the antimicrobial potential of κ-carrageenan-HPM-based composite films for enhanced food safety applications. These functionalized nanofillers will not only improve the physicomechanical and thermal properties of NCP but also enhance their antimicrobial potential against various spoilage microorganisms of meat and dairy, e.g., *Escherichia coli*, *Pseudomonas aeruginosa*, *Listeria monocytogenes*, and *Staphylococcus aureus*. Overall, these nano-active packaging films may provide an alternative strategy to improve the shelf life and safety of poultry (chicken filet) and dairy products (cheese slices).

Materials and Methods

Materials

Rhamnolipids (R90) were purchased from AGAE Technologies (USA). Phosphate buffer saline and) κ-carrageenan was purchased from Sigma-Aldrich (Germany). Hydroxypropyl methylcellulose (HPMC) and glycerol were purchased from Daejung chemicals (South Korea). Nutrient broth, Muller Hinton, and brain heart infusion (BHI) broth/agar were purchased from Merck (USA). Nisin Z was purchased from Honghao Chemical Co. (Shanghai, China). Purified soy lecithin (phosphatidylcholine ⩾ 94%) was provided by Lipoid (Ludwigshafen, Germany).

Fabrication of Rhamnosomes

Rhamnolipids (RLs) functionalized liposomes were prepared according to the method previously described by Niaz et al. (2019) with slight variations. Briefly, 0.5% of phospholipids (soy-lecithin) and RLs were dissolved separately in phosphate buffer saline (PBS, pH 7). Mix the two solutions in 1:1 (v/v) and the mixture was heated at 40 °C in a water bath shaker for 10 min. Rhamnosomes (RS-NCS) were obtained by ultra-sonication of the above mixture for 20 min at 25 kHz. Nisin-loaded nano-vesicles were prepared by dissolving 1 mg/mL of nisin in PBS followed by 30 min of stirring before the addition of phospholipid.

Size and Zeta Potential of Void and Nisin-Rhamnosomes

Size, zeta, and polydispersity index (PDI) of void and active rhamnosomes were determined by dynamic light scattering (DLS) method by using Zeta-sizer (Nano-ZS, Malvern, UK). This instrument works on the principle of dynamic light scattering (DLS). It comprises of 4 mW He/Ne laser, photo multiplier, measurement cell, and correlator. Briefly, 1 mL suspension of RS-NCS was diluted (50 ×) with dH_2O and analyses were performed with a fixed detector angle of 90° and refractive index value 1.49 as described previously (Niaz et al., 2019). Each sample was measured in triplicate and the average values were used.

Preparation of Biopolymeric Coatings

Film-forming solutions (FFS) were prepared by dissolving HPMC (6% w/v) and κ-carrageenan (0.7% w/v) separately in dH_2O. The solutions were mixed (1:1) for 40 min at 65 °C using a heating magnetic stirrer (Fisher Bio-block scientific). To obtain non-active (control packaging) and active food packaging (AP), selected amounts of glycerol (25% w/w) and nisin (1 mg mL^{-1}) were added during stirring. For the nano-active packaging (NAP), void and nisin-loaded rhamnosomes solutions were added separately to double concentrated FFS of HPMC:CR (H-C) blend to obtain a final concentration of 6% for HPMC and 0.7% CR. Finally, NCP films were obtained by pouring approximately 8 g FFS in the Petri-dishes (NEST Biotechnology) and left to dry at room temperature (25 °C) and relative humidity (~50%) for 24–48 h. Dried packaging films were stored in airtight plastic jars with silica beads for further characterization.

Characterization of Nano-Active Packaging

Scanning Electron Microscopy (SEM)

The cross-sectional morphologies of the nano-active packaging films were observed using field emission scanning electron microscope (FE-SEM) (Tescan, USA). Dried NAP was dipped in liquid nitrogen and then cracked with the help of tweezers. A small section of cracked NAP was fixed on conductive SEM sample stubs with double-sided tape and coated with carbon. FE-SEM was operated at an accelerated voltage of 10 kV (Tibolla et al., 2019).

Optical Properties of Nano-Active Packaging

The light barrier properties of H-C coatings were evaluated by exposing packaging to the light source in UV/VIS spectrophotometer (Multiskan GO–Thermo Scientific) and the transmittance of light was measured at 600 nm as described previously (Cui et al., 2017). Briefly, 2 cm × 1 cm (length × width) section of each packaging film was carefully cut with a sterilized surgical blade. Then each section was placed separately in the glass cuvette and optical density at 600 nm was observed using a UV/VIS spectrophotometer. Finally, opacity of prepared coatings was calculated by the following equation:

$$Op = \frac{Abs600nm}{x} \quad (1)$$

where Abs600 is the absorbance at 600 nm and x is the film thickness (mm). Three replicates of each coating were tested.

Fourier Transform Infrared (FTIR) Spectroscopy

Fourier transform infrared (FTIR) spectroscopy analyses of NAP were performed to determine the chemical composition and functional groups present in composite packaging. In addition, the interaction of nanofillers with the biopolymeric matrix of the films was observed. FTIR spectrum of each packaging film was recorded on PerkinElmer 100-FTIR, Italy. Briefly, dried packaging films were cut into 3 cm × 3 cm pieces and then placed on the diamond ATR crystal stage

exposing IR rays. The corresponding spectrum bands were obtained in the wavelength range of 4000–500 cm^{-1} with the spectral resolution of 1 cm^{-1} (Marín-Silva et al., 2019).

Thermogravimetric Analysis (TGA)

To determine the thermal stability of NAP, thermogravimetric analyses (TGA) were performed by using TGA-50 thermal analyzer (Shimadzu, Japan). Approximately 25 mg of sample was weighed in an aluminum crucible pan and subjected to TGA analysis with a temperature range of 50–600 °C. Temperature scans of the samples were carried out under dynamic nitrogen atmosphere (20 cm^3/min) with a heating rate of 10 °C/min. Mass loss was observed as thermal decomposition of the sample occurs with increasing temperature (Niaz et al., 2018).

Differential Scanning Calorimetry (DSC)

To determine the phase transition of various food packaging materials, differential scanning calorimetry (DSC) analyses were performed by using DSC-50 (Shimadzu, Japan), equipped with STARe software. Approximately 25 mg sample was weighed in an aluminum pan. Each calorimetric pan was sealed and subjected to DSC analysis, with a heating range from − 30 to 50 °C with 10 °C/min increase in temperature under the nitrogen flow of 20 cm^3/min (Swaroop & Shukla, 2019). Empty aluminum pans were used as control. Samples were run in triplicate to check the reproducibility of the results.

Mechanical Properties of Nano-active Packaging

Film thickness was measured using a 0–25-mm manual micrometer, with a resolution of 0.01 mm. The reported values were the average of 6 readings taken randomly on each coating.

The mechanical characteristics of NAP were evaluated by tensile strength (TS, MPa), Young's modulus (YM), and ultimate elongation (UE, %) using an electronic universal tensile machine (UTM 6203). Packaging films (section of 50 mm × 20 mm (analyzed area = 30 mm × 20 mm)) were uniaxially stretched in the vertical direction at a constant speed of 10 mm/min (Kamkar et al., 2021). The obtained data were then used to calculate the TS and UE of the film samples according to the following equations:

$$TS(MPa) = \frac{\text{Load on the film causing it to break (N)}}{\text{Cross section of the film (mm2)}} \quad (2)$$

$$UE\ (\%) = [Elongation\ at\ break \div Initial\ gauge\ length] \times 100 \quad (3)$$

Antimicrobial Potential of Non-active, Active, and Nano-active Coatings

The growth kinetics of foodborne bacterial strains were tested under the influence of various film-forming solutions (FFS) of different formulation. Optical density values of inoculated broth containing FFS of non-active, active, and nano active packaging (NAP) were recorded at 595 nm in 96-well plates by using Multiskan™ GO Microplate Spectrophotometer for 72 h.

The qualitative antibacterial potential of the dried NAP films was performed by disk diffusion assay with modifications. Briefly, 1-cm^2 square sections were cut from different composite packaging films and positioned carefully on nutrient agar medium plates, previously inoculated (0.1% v/v) with *Pseudomonas aeruginosa*, *Staphylococcus aureus*, *E. coli*, and *Listeria monocytogenes* separately. Finally, the plates were incubated at 37 °C for 24 h, and the diameters (mm) of the growth inhibition zones were measured.

Food Application Challenge: Antimicrobial Test In Situ

Active, non-active nano and nano-active packaging films were used for direct application on fresh chicken breast filets and cheese slices as described previously (Göksen et al., 2020) with slight modifications. Briefly, 6-g pieces of cheese slice and chicken filets were sterilized with UV light in a laminar flow safety cabinet for 30 min. Subsequently, they were inoculated with 100 µL of overnight bacterial culture (10^5 CFU/mL) separately and spread with a sterile swab. The inoculated slices were kept 15 min within the laminar flow safety cabinet to let the food surface absorb the inoculum and then covered the inoculated side with sterile packaging films (4 × 4 cm) and placed in sterile polyethylene zip bags. Each treatment was tested in triplicate under refrigerated storage conditions for 18 days. Uncoated food samples were used as positive controls and control packaging films (without nisin and NCS) were also used for comparison.

Results and Discussion

Characteristics of Rhamnosomes Nanocarrier

To determine the hydrodynamic size of the RS-NCS, dynamic light scattering (DLS) technique was used. Void and active non-functionalized liposomes exhibited a mean diameter of 144 ± 6 nm and 160 ± 4 nm, respectively (data not presented). On the other hand, the mean diameter of

void and active (nisin-loaded) RS-NCS was 209 ± 6 nm and 293 ± 2 nm, respectively. As observed in Fig. S1 (supplementary data), the particle size was increased after stabilization with biosurfactant, which is in coherence with the previous reports (Aboumanei et al., 2021; Gorjian et al., 2021). After the encapsulation of bioactive agent (nisin) in RS-NCS, particle size further increased. Similar results were observed previously while studying polysaccharide stabilized nanoliposomes (Seyedabadi et al., 2021). Polydispersity index (PDI) values were found to be 0.37 and 0.38 in both void and active RLs functionalized liposomes (rhamnosomes) respectively, which indicated a homogeneous distribution of functionalized NCS.

ζ-potential is an important measurement to confer stability of any NCS, and zeta potential values above ± 30 mV usually indicate the dispersion stability of NCS by preventing aggregation and fusion between the particles (Jain et al., 2021). ζ-potential of RS-NCS was − 35.5 ± 11.9 mV, which confirms the stability of liposomes after functionalization with anionic surfactant RLs. After encapsulation of nisin, the zeta potential was reduced to − 20 mV, due to the cationic nature of nisin. These results also indicate that nisin not only encapsulates inside the core of NCS but is also anchored on the surface of RS-NCS by adsorption. This could be due to the electrostatic interactions between the oppositely charged peptide and RS-NCS.

Physico-Mechanical and Thermal Characterization of Packaging Films

Cross-section Analysis of Packaging Films

The effect of RS-NCS (rhamnosome nano-carrier systems) on the internal structure of the H-C coatings was observed with SEM. Cross-section images of the selected packaging could be seen in Fig. 1A. Non-active composite packaging films presented a non-porous, dense, compact, and rough morphology (Fig. 1A (I, II)), which can be attributed to the high matrix chain interaction between the two polymers via electrostatic and H-bonding. Furthermore, in Fig. 1A (III, IV), uniform distribution of NCS can be observed. The uniform distribution of non-active and active RS-NCS across the polymer matrix can be associated with low interaction between polymer chains due to the formation of convoluted paths in the polymer matrix. Moreover, mechanical and thermal properties of polymer-based packaging films are mainly determined by the degree of dispersion of NCS in the polymeric matrix. Homogeneous distribution of NCS in the polymer matrix can improve the mechanical and thermal stability of packaging films (Hasheminya et al., 2018; Jafarzadeh & Jafari, 2020). This is in accordance with our results (mentioned in the previous sections), where mechanical and thermal properties of the H-C coatings were enhanced by the addition of RS-NCS (rhamnosomes) and are associated with the uniform distribution of RS-NCS in the polymer matrix.

Optical Properties of Packaging Films

The optical properties of nano-active packaging (NAP) are important for its consumer acceptability. Figure 1B illustrates the optical properties of non-active, active as well as non-functionalized (liposomes) and functionalized (rhamnosomes) nanofiller-embedded packaging materials. NAP incorporated with functionalized nanofillers (RS-NCS) are more transparent (low opacity) than NAP with non-functionalized nanofillers (liposomes). This can be attributed to higher turbidity and yellowness of soy-lecithin (liposomes), hence more refraction or reflection of light occurred, which resulted in higher opacity of NAP having non-functionalized nanofillers. However, RS-NCS embedded NAP was less transparent (high opacity) than control packaging films (without nanofillers). It was observed previously that the addition of nanofillers reduced the transparency of polymeric films (Motelica et al., 2020) as these nanocarriers systems (NCS) embedded inside the polymeric matrix, make the polymeric film more dense, and act as a physical hindrance to light. Hence, less light will pass through the packaging films which would result in low transparency of NAP than non-active control packaging films.

Fourier Transform Infrared (FTIR) Spectroscopic Analysis

From the FTIR spectrum of HPMC, the characteristic peaks were observed at 3468 cm^{-1}, 2932 cm^{-1}, and 1064 cm^{-1} attributing to the stretching vibration of O–H, H-C symmetric or asymmetric vibrations of CH_3 and C-O groups, respectively (Fig. 2I). The bands at 1647 cm^{-1}, 1462, and 1378 cm^{-1} were assigned to water in the amorphous region and CH bending or C-COO stretching respectively. In-plane and out of plane bending of C = O appeared at 612 cm^{-1} (Wrona et al., 2017).

In the spectrum of carrageenan powder (Fig. 2II), peaks at 2926 cm^{-1} and 1583 cm^{-1} represent O–H and sulfate stretch, respectively. The peaks at 1049 cm^{-1} and 916 cm^{-1} and a clear band at 849 cm^{-1} are attributed to the glycoside linkage, 3, 6-anhydro-D-galactose and sulfate at the C4 position in the galactose ring, respectively (Paula et al., 2015; Polat et al., 2020).

The FTIR spectra of non-active (H-C blend) coatings (Fig. 2III) revealed the bands at 3303 cm^{-1} and 2931 cm^{-1}, which were confirmed as O–H stretching and C-H stretching, respectively. The C-O stretching from 1000 to 1200 cm^{-1} represented primary and secondary alcohol in κ-CR

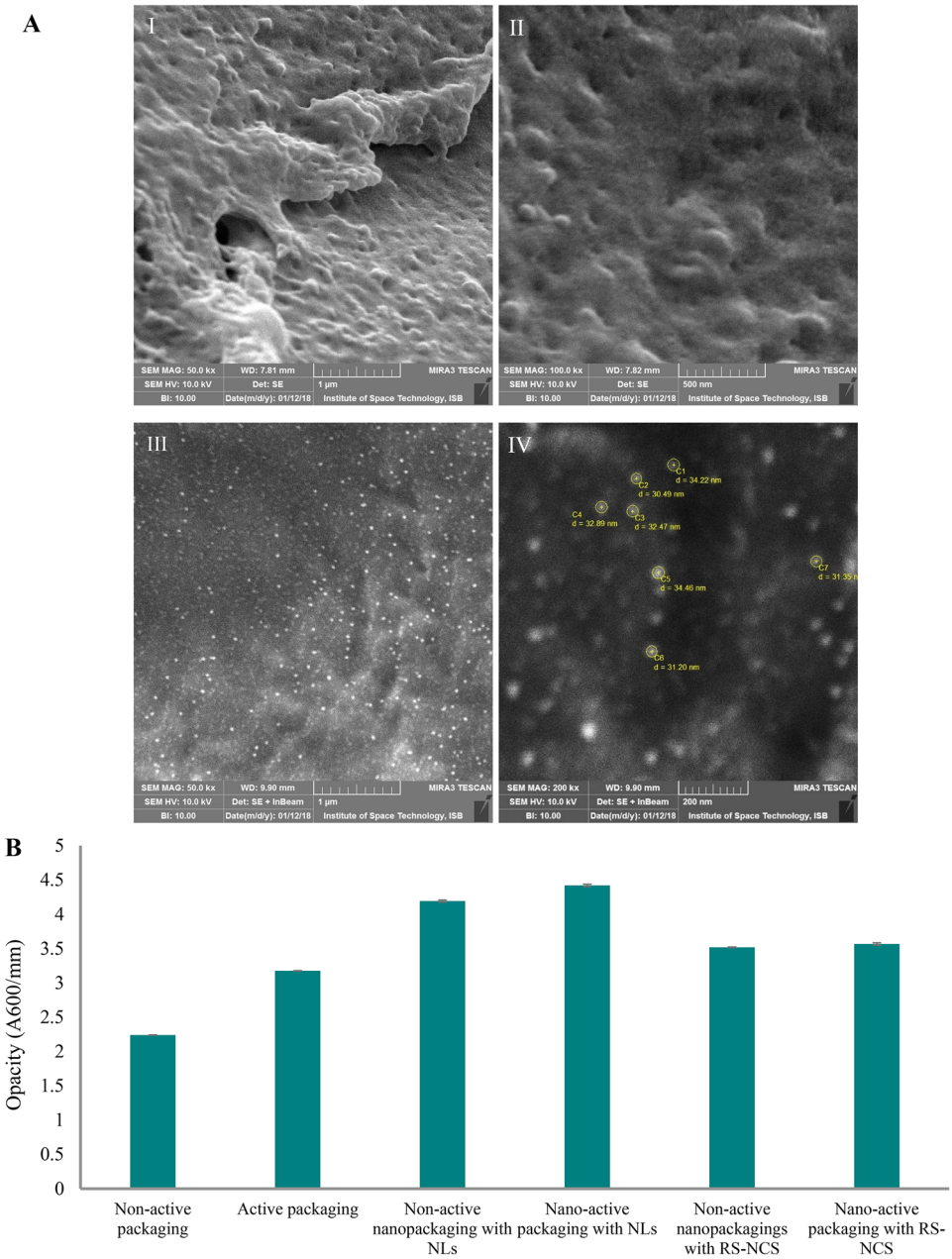

Fig. 1 **A** Cross-section images of HPMC and κ-carrageenan based non-active composite packaging (I and II) and nano-active packaging with RS-NCS (III and IV) observed under scanning electron microscopy at different resolution. **B** Opacity of different non-active (H-C blend packaging), active (containing free nisin), non-active nano (containing void NCS), and nano active coatings (with active NCS) recorded at 600 nm as (Opacity = OD at 600 nm/thickness in mm)

and HPMC. The bands at 1375 cm^{-1}, 1036 cm^{-1}, 925 cm^{-1}, and 832 cm^{-1} are corresponding to sulfate ester, glycosidic linkages, 3, 6-anhydrogalactose, and galactose-4-sulfate ester in κ-carrageenan, respectively (Balqis et al., 2017). The appearance of a new peak at 2120 cm^{-1} is attributed to the C-H stretch of alkanes from the aliphatic chain of glycerol, which demonstrated good miscibility of glycerol with packaging polymers. Slight shift in all characteristic bands of nano-active (NAP) and non-active nano packaging (Fig. 2V and VI) indicated the embedding of RS-NCS inside the polymer network without any chemical interaction.

Thermogravimetric Analysis

Thermogravimetric analyses (TGA) were performed to determine the thermal behavior and the influence of RS-NCS with or without an active agent on the thermal stability of the prepared nano-active packaging (NAP) films. The samples of non-active (H-C polymer blend) films suffer a small loss of mass at the beginning of heating till 89.2 °C, indicating the presence of water (Fig. 3A (I)) in κ-carrageenan (κ-CR) owing to its gelation property. Second mass loss curve until 226.2 °C represented degradation/decomposition of κ-CR, with nearly 37.5% mass loss. Second mass loss peak in TGA

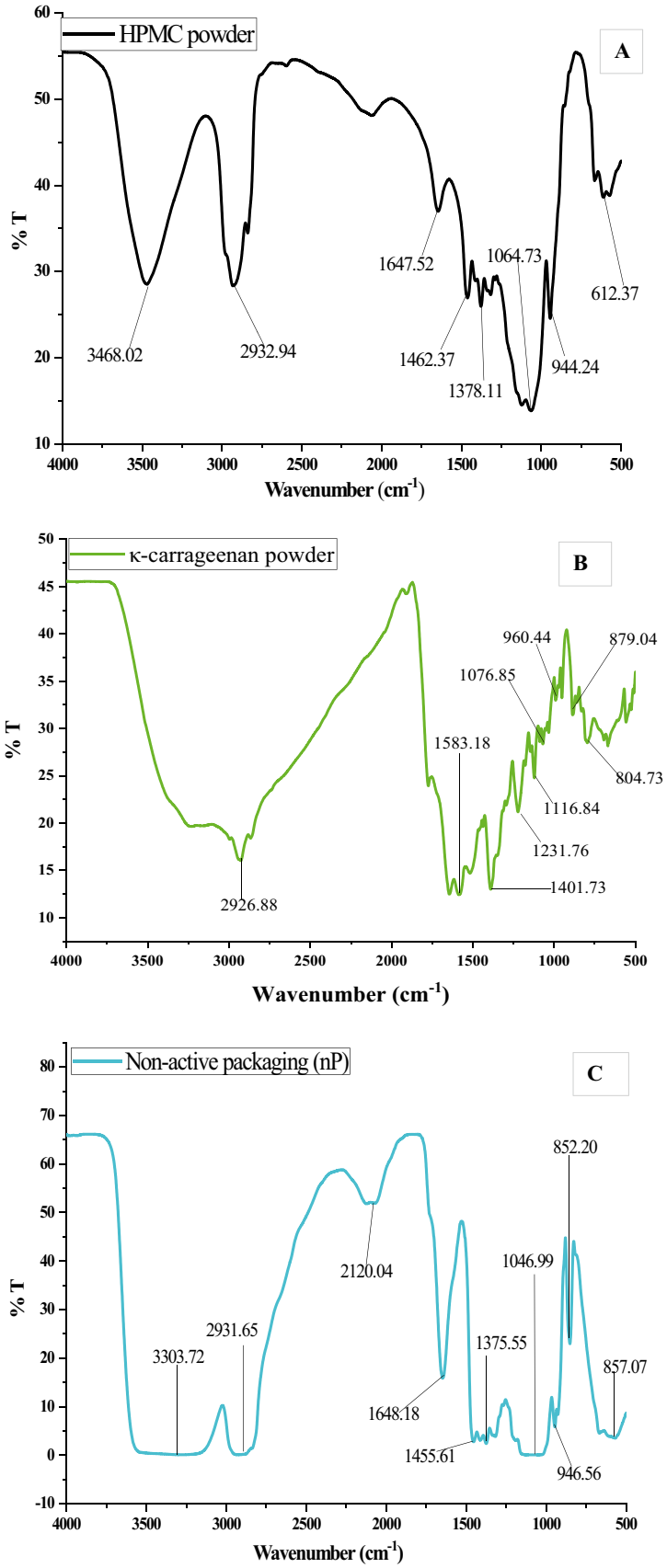

Fig. 2 Fourier transform infrared spectral analysis of HPMC powder (**I**), Carrageenan powder (**II**), non-active packaging (H-C blend) (**III**), active packaging (**IV**), non-active nano packaging (**V**), and nano-active packaging (**VI**)

Fig. 2 (continued)

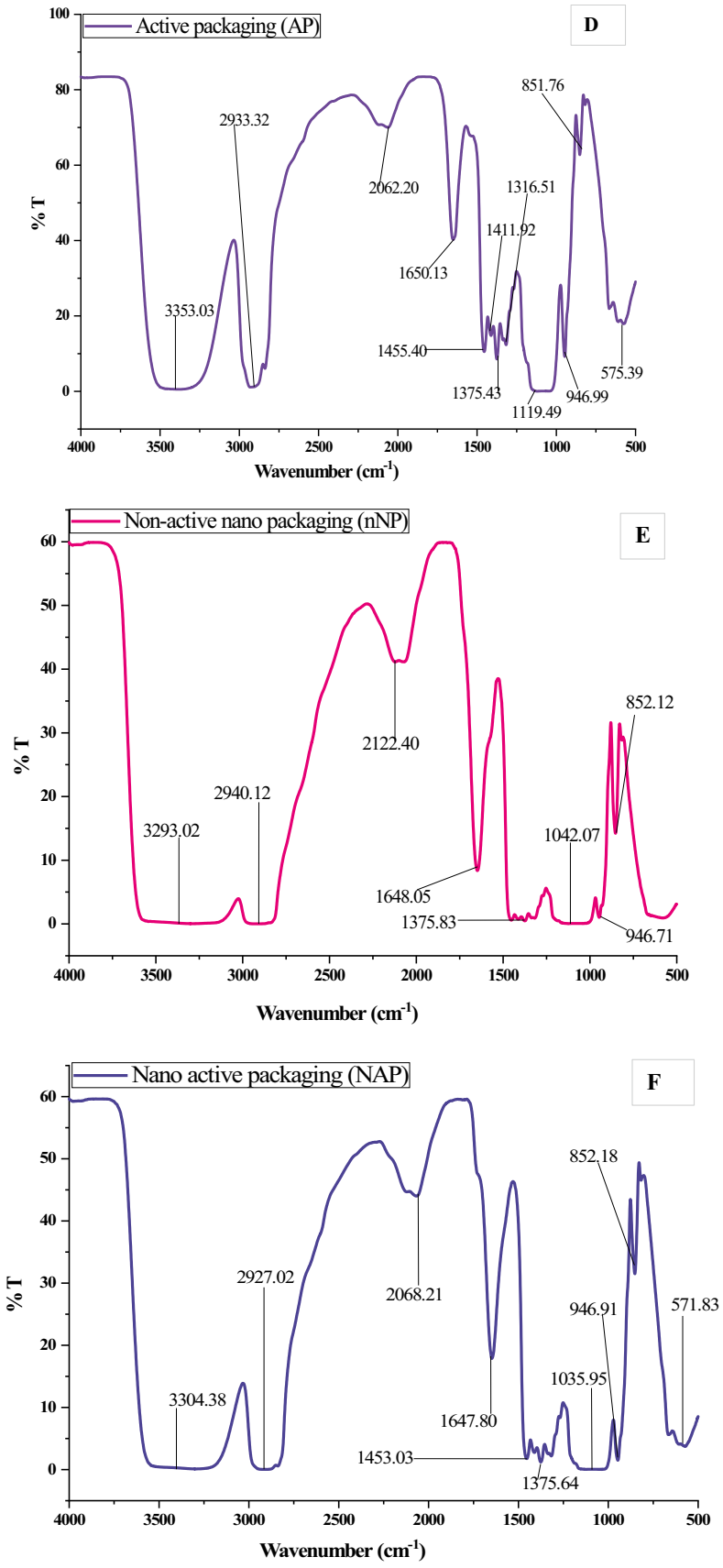

curve of non-active packaging films represented 20% mass loss until 353 °C and it was attributed to HPMC decomposition. On the other hand, after incorporating void liposomes in nano non-active packaging films, only 8% mass loss till 200 °C and 64% of mass loss was observed above this temperature, whereas 33% of mass loss was observed with RS-NCS. Similar behavior was detected for nano-active packaging films with nisin-loaded RS-NCS (Fig. 3A (II)), since they suffer a small loss of mass till 400 °C, indicating the presence of less water. Comparable results were observed previously where the addition of active agent-loaded nano-carrier systems increased the thermal stability of food packaging films (Jafarzadeh & Jafari, 2020). These results confirmed that nano-active packaging films prepared with void and nisin-loaded functionalized NCS were thermally stable even above 200 °C and adequate for most food-packaging applications.

Differential Scanning Calorimetric (DSC) Analysis

DSC analysis allows us to determine the glass transition temperature (Tg), melting points (Tm), and relative crystallinity (Xc) of non-active packaging (control), active packaging, and nano-active packaging (NAP). DSC thermograms of all variants are presented in Fig. 3B (I and II). Previously, it was observed that the addition of nano-carrier systems (NCS) to the HPMC matrix decreased the melting temperature of HPMC coatings. Conversely, the melting enthalpies of each of the HPMC coatings containing NCS were always higher

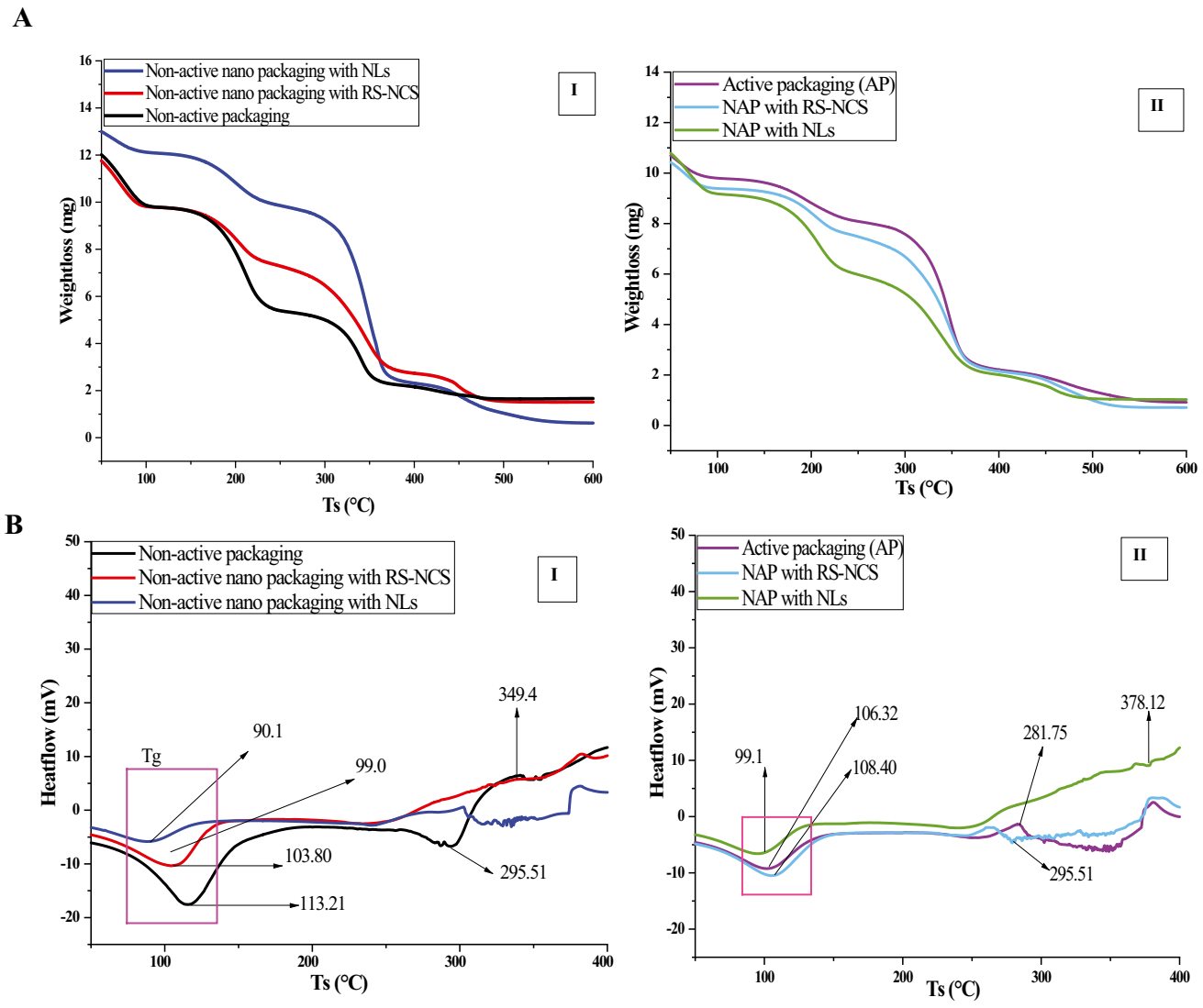

Fig. 3 **A** Thermogravimetric analysis (TGA) of non-active nanocomposite packaging as well as non-active packaging (I), and TGA curves of active packaging and nano-active packaging (II). **B** Differential scanning calorimetric (DSC) analysis of antimicrobial active and nano-active coatings (I), and non-active nanocoatings (II)

than that of the neat HPMC coatings (Wrona et al., 2017). Glass transition (Tg) of pure HPMC coatings ranges between 132 and 230 ℃ due to its amorphous nature. On the other hand, Tg of raw κ-carrageenan powder appears above 100 °C (Alnaief et al., 2018). The moisture desorption peak, due to the hydrophilic nature of carrageenan, is reported as sol–gel transition temperature in literature. "Tg" peak was not much evident after the addition of plasticizers in κ-carrageenan, possibly due to the decrease in intermolecular forces of polymers by water and plasticizers during the preparation of packaging films. Similar results were obtained previously (Balqis et al., 2017).

In the control packaging films (HPMC-carrageenan blend), "Tg" was observed at 113.2 °C, which was attributed to the crosslinking between two polymers. Aerogel forming capability by κ-carrageenan reduces the amorphous character of HPMC, which resulted in reduced Tg of blend H-C packaging films. Another endothermic peak was observed at 295 °C, which is attributed to κ-carrageenan melting and decomposition with the fragmentation and breakdown of the carbohydrate backbone. Similarly, a small endothermic peak at 349.4 °C (Tm) represented the decomposition of HPMC polymer. Previously thermal decomposition of HPMC was observed from 210 °C to 423.2 °C (Dharmalingam & Anandalakshmi, 2019). After the incorporation of void nanoliposomes and rhamnosomes, Tg of non-active nano packaging reduced from 113.2 to 90.1 °C and 103.8 °C, respectively. Nevertheless, after incorporating nisin-loaded NCS (nano-active coatings), a slight increase in Tg (99.1 °C and 108.40 °C) was observed. In active packaging, Tm appeared at 281.7 °C; however, this Tm peak disappeared in NAP (Fig. 3B (II)) owing to less amorphous and more lipid content of NAP in the form of rhamnolipids (RL) and phospholipids (PL). It was observed previously that higher values of Tg and Tm represent stronger intermolecular bonds between polymer chains (Shiroodi et al., 2016). On the other hand, lower Tg can be correlated to the increase of tensile strength (TS), where polymer interaction with NCS induced compactness of the films (Ili Balqis et al., 2017). Overall, we can conclude that the NAP having rhamnosomes based nanofillers are thermally more stable than the non-active as well as non-functionalized nanofillers (liposomes) containing films.

Mechanical Properties of Non-active, Active, and Nano-active Packaging Films

Mechanical properties depend on the composition and nature of packaging components. These properties are important when the packaging films are intended to withstand external stress while maintaining the integrity (Hosseini et al., 2013). The measurement of these properties allows predicting how the material will behave under different food processing conditions. Tensile strength (TS), Young's modulus (YM), and elongation (E) are important mechanical properties to evaluate the strength and flexibility of bioactive coatings and are presented in Table 1. These mechanical properties were also influenced by the incorporation of the nano-carrier systems and active agents in the packaging films. Adding free nisin lowered the TS and %E and slightly increased the YM of the HPMC-carrageenan-based packaging than the control H-C-based packaging without an active agent. This reduction in mechanical property of packaging could be due to disturbance in the interaction of polymer chains of HPMC and carrageenan by nisin molecules in the mesh network, which may weaken the structure and hence decrease the TS of the emulsified coatings (Klangmuang & Sothornvit, 2016).

Similarly, after incorporation of nano-liposomes and rhamnosomes; TS, YM, and %E increased than the packaging films containing free nisin. Lipid-based NCS interfere with the hydrogen bonding of bioactive coatings, reducing their rigidity and resistance while increasing their extensibility. On the other hand, nisin owing to its more amorphous nature increased the rigidity of the packaging film, which reduced the mechanical strength (Motta et al., 2020). Similar results have been reported previously, where the addition of polymeric NCS improved the mechanical properties of the bioactive coatings (Hasheminya et al., 2018; Jafarzadeh & Jafari, 2020).

Antibacterial Activity of Non-active, Active, and Nano-active Packaging

Time-kill assay was performed to evaluate the antibacterial activities of HPMC and κ-CR-based active packaging films incorporated with nisin against gram-negative

Table 1 Tensile strength (TS), young modulus and elongation at break (EB) of non-active, active and nano active composite coatings. All values were expressed as mean ± standard error ($n = 3$)

Mechanical characteristics of NAP	Non-active packaging	Active packaging with free nisin	NAP with void liposomes	NAP with loaded liposomes	NAP with void RS-NCS	NAP with loaded RS-NCS
Tensile strength (MPa)	3.90 ± 0.05	2.96 ± 0.03	3.50 ± 1.34	3.12 ± 0.09	5.38 ± 0.04	5.16 ± 0.06
Young modulus (MPa)	1086 ± 0.95	1107 ± 0.67	1562 ± 0.50	1785 ± 0.71	1566 ± 0.66	2777 ± 0.77
Elongation (%)	1.95 ± 0.02	1.48 ± 0.06	1.75 ± 0.01	1.56 ± 0.04	2.69 ± 0.01	2.58 ± 0.03

(*Pseudomonas aeruginosa* and *E. coli*) and gram-positive (*S. aureus* and *L. monocytogenes*) bacteria (Fig. 4A–D). Rhamnolipids and nisin both are well-known antimicrobial agents against foodborne pathogens (Chen et al., 2019). Non-active film-forming solution (FFS) did not exhibit significant antimicrobial activity against all foodborne bacteria used in this study. A slight reduction in the bacterial growth in the presence of non-active FFS could be due to gelling property of κ-CR in the aqueous medium, which reduced the oxygen and nutrients supply to pathogens and decreased the bacterial growth (Niaz et al., 2018; Zhu et al., 2017). Similarly, active FFS with free nisin remained inactive against gram-negative pathogens, e.g., *P. aeruginosa* and *E. coli* (Fig. 4A and C), as its antimicrobial activity is solely against gram-positive bacteria. The outer membrane in gram-negative bacteria acts as a permeability barrier and prevents nisin from pore formation (Aljasir et al., 2020). However, non-active nano and nano-active FFS incorporated with rhamnosomes (RS) NCS not only reduced the gram-negative (*P. aeruginosa* and *E. coli*) bacterial growth but also significantly controlled the gram-positive (*S. aureus* and *L. monocytogenes*) bacteria for 72 h. RS-NCS controlled the bacterial growth because of rhamnolipids in its structure, which demonstrated a permeabilizing effect, thus leading to the disruption of the cellular membrane. In a recent study, it was observed that the hydrophobic character of RL favors its penetration into gram-negative cells as well (de Freitas Ferreira et al., 2018), thus resulting in broad-spectrum antimicrobial activity.

Furthermore, to estimate the antimicrobial efficacy of different packaging films against foodborne bacteria, a modified disk diffusion assay was performed. This method is based on the release of nisin from intrinsically active RS-NCS present inside the packaging material disk, which generates an inhibition zone on a pre-inoculated agar medium after overnight incubation (Khodayari et al., 2019). Inhibitory zones of non-active packaging as control, AP, and NAP with functionalized and non-functionalized liposomes are presented in Fig. S2. NAP with void and loaded RS-NCS exhibited efficient antimicrobial activity against all tested bacteria. This high efficacy of NAP embedded with void RS-NCS could be due to the broad-spectrum antimicrobial activity of rhamnolipids in functionalized liposomes, which make RS-NCS intrinsically active against tested bacterial strains. Correspondingly, NAP with nisin-loaded RS-NCS demonstrated even better control against tested microbes, owing to the synergistic effect of nisin and RS-NCS. The

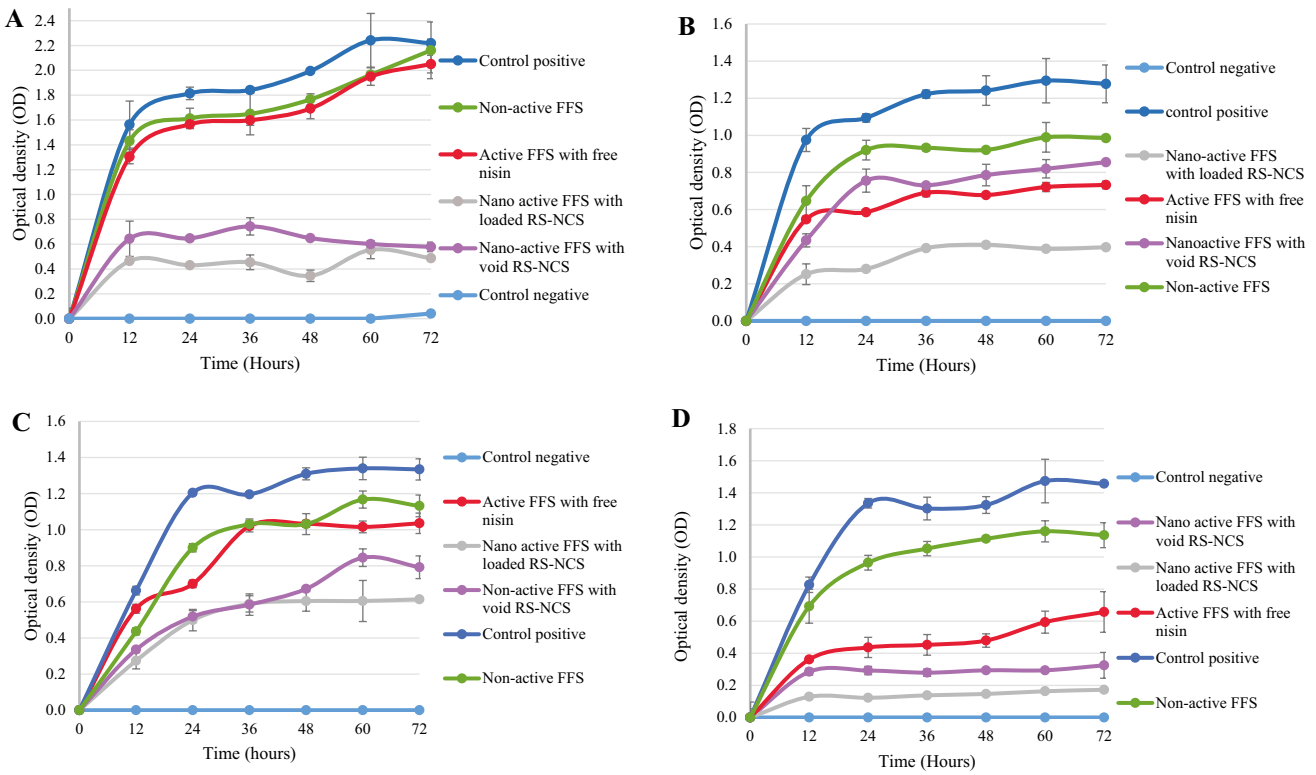

Fig. 4 Time kill assay of various non-active, active and nano-active packaging films against *Pseudomonas aeruginosa* (**A**), *Staphylococcus aureus* (**B**), *E. coli* (**C**), and *Listeria monocytogenes* (**D**)

addition of nisin in intrinsically active NCS, which were further embedded in the biopolymer matrix caused greater inhibition zones against the tested bacterial strains. Antimicrobial activity of different nano-composite films against food spoilage microorganisms has been reported previously (Bahrami et al., 2019).

Active packaging (AP) demonstrated better activity against gram-positive bacteria, i.e., *S. aureus* and *L. monocytogenes* (Fig. S2B and D) than gram-negative bacteria, i.e., *P. aeruginosa* and *E. coli* (Fig. S2A and C). The observed difference in the antimicrobial activity of active packaging (containing free nisin) was due to the inactivity of nisin against gram-negative pathogens. However, many authors have suggested that nisin can establish broad-spectrum antimicrobial activity when used in combination with other antimicrobial agents, e.g., lysozymes and EDTA (Heesterbeek et al., 2019; Lopes et al., 2019).

Food Application Challenge: Antimicrobial Test In Situ

To assess the application potential of RS-NCS embedded active packaging films, quantitative bacterial count assays on cheese slices and chicken filets were carried out under refrigerated storage conditions. For comparison purposes, control packaging (without nisin and NCS), active packaging (with free nisin) and non-active packaging films (having void RS-NCS) were also prepared and tested. The antimicrobial efficacy of packaging films against *L. monocytogenes* and *E. coli* inoculated on cheese slices are shown in Fig. 5A and B; whereas the antimicrobial effect against meat pathogens, i.e., *S. aureus* and *P. aeruginosa* are presented in Fig. 5C and D.

For control packaging (without nisin and NCS), *Listeria monocytogenes* remained viable without any significant reduction in the number of viable cells after 18 days

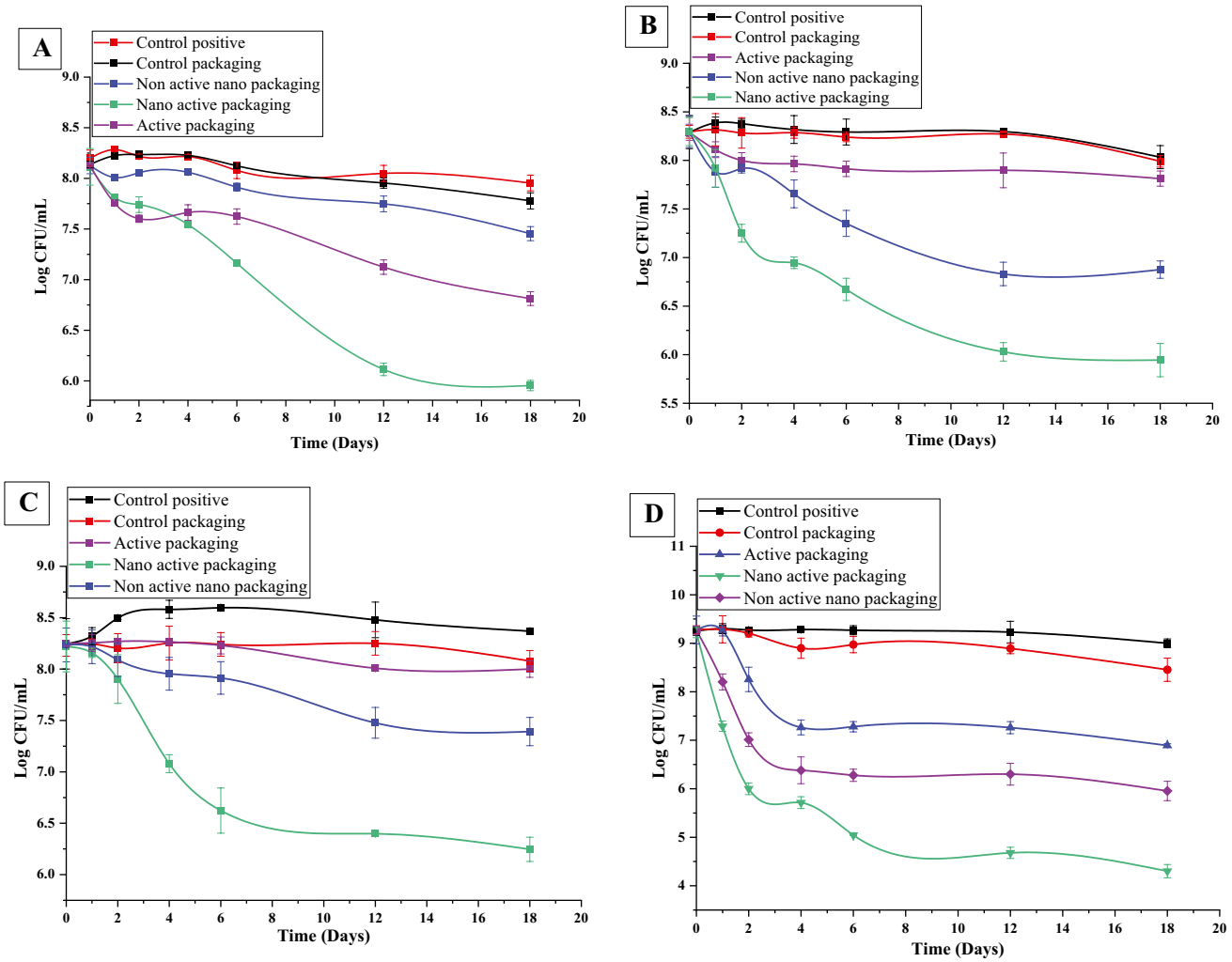

Fig. 5 Food application assay to improve the shelf life of milk and meat products: Quantitative antibacterial activity of active and nano-active packaging on cheese slices inoculated with *L. monocytogenes* (**A**) and *E. coli* (**B**), and on chicken breast filets inoculated with *Pseudomonas aeruginosa* (**C**) and *Staphylococcus aureus* (**D**) under refrigerated storage condition

(Fig. 5A). Immediately after application of the active packaging (with free nisin), a significant reduction from 8.1 to 7.2 log CFU/g and a continuous decrease in the bacterial count was observed, until the last day of storage. Nano-active packaging demonstrated the best control against *Listeria monocytogenes* on cheese slices and overall, 2.1 log unit reduction was recorded during the studied period. Conversely, after application of the non-active nano packaging embedded with void RS-NCS on cheese, only one log unit reduction was observed for *Listeria monocytogenes* during refrigerated storage.

Concerning the growth of *E. coli* (Fig. 5B) on cheese slices, during first 4 days, 0.5, and 2.5 log unit reduction in *E. coli* count was observed when treated with active and nano-active packaging, respectively. Similarly, non-active nanopackaging demonstrated better activity against *E. coli*, as a significant decrease in bacterial count (from 8.2 to 6.8 log CFU/g) was observed. These results demonstrated that the incorporation of RS-NCS in the C-H films made them intrinsically active (antimicrobial) to reduce the bacterial count. The broad-spectrum antimicrobial activity of RLs in NCS as well as its synergistic effect with nisin in NAP helped to control the bacterial strains more efficiently than active packaging (AP).

For meat-associated pathogens, control packaging films had demonstrated no antimicrobial activity. Similarly, AP could not demonstrate a considerable antimicrobial action against gram-negative bacteria when compared to the gram-positive ones, owing to the inactivity of nisin against gram-negative pathogens. However, during storage period, treatment with nisin-loaded RS-NCS displayed significantly lower counts of *P. aeruginosa* than the control (Fig. 5C), indicating that, though milder, the presence of rhamnolipids and nisin in the polymer matrix exerted antimicrobial activity against *P. aeruginosa*.

For inoculated chicken breast filets with *Staphylococcus aureus* (Fig. 5D), even after 4 days of incubation, the efficacy of nano-active packaging with loaded RS-NCS was considerably more evident than the active packaging. As NAP reduced the bacterial count by almost double (4.5 log unit reduction) than the active packaging (almost 2 log unit reduction). It is worthy to notice that initially AP slightly inhibited the growth of Gram-positive meat pathogen, but after 4 days, no further reduction in the bacterial count was observed. The fast release of nisin from the AP rapidly reduced the bacterial count, but then the effect was diminished. After 18 days of refrigerated storage, NAP showed lower bacterial counts than the packaging films with free nisin. Though both formulations were containing the same concentration of nisin, the nanostructures had a significant impact in terms of sustained release of antimicrobials. These findings suggested the effectiveness of the encapsulation process to prolong the release of the active compounds. Furthermore, nanoencapsulation reduced the activity loss of free nisin due to inactivation in complex food systems (Santos et al., 2018). Meaningful results obtained in situ justify that NAP reinforced with nisin-loaded rhamnolipids functionalized NCS can increase the shelf life of milk and meat-based products by preventing post-processing bacterial contaminants.

Conclusion

Rhamnolipids functionalized nanofillers (RS-NCS) improved the thermal stability, transparency, and mechanical properties of the nano-active packaging (NAP) as compared to active packaging (AP). Furthermore, RS-NCS incorporated in the composite coatings demonstrated strong antibacterial activity against both gram-positive and gram-negative foodborne bacteria. During application study on the real food systems (chicken filets and cheese slices), it was observed that packaging films reinforced with nisin-loaded RS-NCS were more effective in inhibiting the growth of foodborne bacteria when compared with active and control packaging films under refrigerated storage conditions Thus, here, reported innovative NAP can have potential applications as functionalized food packaging solution to extend the shelf life of dairy and poultry products. In future, controlled release kinetics of active agents from nanofillers, AP, and NAP would be investigated in detail for better prediction of the shelf-life of packaged food products.

Supplementary Information The online version contains supplementary material available at https://doi.org/10.1007/s11947-022-02815-2.

Funding This work was supported by the Higher Education Commission, Pakistan (NRPU grant No. 20–4260/R&D/HEC/14/127).

Data Availability Data will be made available on reasonable request.

Declarations

Competing Interests The authors declare no competing interests.

References

Aboumanei, M. H., Mahmoud, A. F., & Motaleb, M. (2021). Formulation of chitosan coated nanoliposomes for the oral delivery of colistin sulfate: In vitro characterization, 99mTc-radiolabeling and in vivo biodistribution studies. *Drug Development and Industrial Pharmacy, 47*(4), 626–635.

Aljasir, S. F., Gensler, C., Sun, L., & D'Amico, D. J. (2020). The efficacy of individual and combined commercial protective cultures against Listeria monocytogenes, Salmonella, O157 and non-O157 shiga toxin-producing Escherichia coli in growth medium and raw milk. *Food Control*, *109*, 106924.

Almasi, H., Jahanbakhsh Oskouie, M., & Saleh, A. (2020). A review on techniques utilized for design of controlled release food active packaging. *Critical Reviews in Food Science and Nutrition*, 1–21.

Alnaief, M., Obaidat, R., & Mashaqbeh, H. (2018). Effect of processing parameters on preparation of carrageenan aerogel microparticles. *Carbohydrate Polymers, 180*, 264–275.

Amjadi, S., Emaminia, S., Nazari, M., Davudian, S. H., Roufegarinejad, L., & Hamishehkar, H. (2019). Application of reinforced ZnO nanoparticle-incorporated gelatin bionanocomposite film with chitosan nanofiber for packaging of chicken fillet and cheese as food models. *Food and Bioprocess Technology, 12*(7), 1205–1219.

Amjadi, S., Nouri, S., Yorghanlou, R. A., & Roufegarinejad, L. (2020). Development of hydroxypropyl methylcellulose/sodium alginate blend active film incorporated with Dracocephalum moldavica L. essential oil for food preservation. *Journal of Thermoplastic Composite Materials*, 0892705720962153.

Aydogdu, A., Yildiz, E., Ayhan, Z., Aydogdu, Y., Sumnu, G., & Sahin, S. (2019). Nanostructured poly (lactic acid)/soy protein/HPMC films by electrospinning for potential applications in food industry. *European Polymer Journal, 112*, 477–486.

Aziz, S. G. –G., & Almasi, H. (2018). Physical Characteristics, Release Properties, and Antioxidant and antimicrobial activities of whey protein isolate films incorporated with thyme (Thymus vulgaris L.) extract-loaded nanoliposomes. *Food and Bioprocess Technology*, *11*(8), 1552–1565.

Bahrami, A., Mokarram, R. R., Khiabani, M. S., Ghanbarzadeh, B., & Salehi, R. (2019). Physico-mechanical and antimicrobial properties of tragacanth/hydroxypropyl methylcellulose/beeswax edible films reinforced with silver nanoparticles. *International Journal of Biological Macromolecules, 129*, 1103–1112.

Balqis, A. I., Khaizura, M. N., Russly, A., & Hanani, Z. N. (2017). Effects of plasticizers on the physicochemical properties of kappa-carrageenan films extracted from Eucheuma cottonii. *International Journal of Biological Macromolecules, 103*, 721–732.

Becerril, R., Nerín, C., & Silva, F. (2020). Encapsulation systems for antimicrobial food packaging components: An update. *Molecules, 25*(5), 1134.

Bigi, F., Haghighi, H., Siesler, H. W., Licciardello, F., & Pulvirenti, A. (2021). Characterization of chitosan-hydroxypropyl methylcellulose blend films enriched with nettle or sage leaf extract for active food packaging applications. *Food Hydrocolloids*, 106979.

Bodbodak, S., Shahabi, N., Mohammadi, M., Ghorbani, M., & Pezeshki, A. (2021). Development of a novel antimicrobial electrospun nanofiber based on polylactic acid/hydroxypropyl methylcellulose containing pomegranate peel extract for active food packaging. *Food and Bioprocess Technology*.

Chen, J., Lü, Z., An, Z., Ji, P., & Liu, X. (2019). Antibacterial activities of sophorolipids and nisin and their combination against foodborne pathogen Staphylococcus aureus. *European Journal of Lipid Science and Technology*.

Chi, W., Cao, L., Sun, G., Meng, F., Zhang, C., Li, J., & Wang, L. (2020). Developing a highly pH-sensitive κ-carrageenan-based intelligent film incorporating grape skin powder via a cleaner process. *Journal of Cleaner Production*, *244*, 118862.

Cui, H., Yuan, L., & Lin, L. (2017). Novel chitosan film embedded with liposome-encapsulated phage for biocontrol of Escherichia coli O157:H7 in beef. *Carbohydrate Polymers., 177*, 156–164.

de Freitas Ferreira, J., Vieira, E. A., & Nitschke, M. (2018). The antibacterial activity of rhamnolipid biosurfactant is pH dependent. *Food Research International*.

de Souza, R. C., de Moraes, J. O., Haberbeck, L. U., de Araújo, P. H. H., Ribeiro, D. H. B., & Carciofi, B. A. M. (2021). Antibacterial activity of low-density polyethylene and low-density polyethylene-co-maleic anhydride films incorporated with ZnO nanoparticles. *Food and Bioprocess Technology., 14*(10), 1872–1884.

Dharmalingam, K., & Anandalakshmi, R. (2019). Fabrication, characterization and drug loading efficiency of citric acid crosslinked NaCMC-HPMC hydrogel films for wound healing drug delivery applications. *International Journal of Biological Macromolecules., 134*, 815–829.

Food & Drug Administration. (2011). *Food additive status list*. Silver Spring, MD, USA: US Food and Drug Administration.

Göksen, G., Fabra, M. J., Ekiz, H. I., & López-Rubio, A. (2020). Phytochemical-loaded electrospun nanofibers as novel active edible films: Characterization and antibacterial efficiency in cheese slices. *Food Control*, *112*, 107133.

Gorjian, H., Raftani Amiri, Z., Mohammadzadeh Milani, J., & Ghaffari Khaligh, N. (2021). Preparation and characterization of the encapsulated myrtle extract nanoliposome and nanoniosome without using cholesterol and toxic organic solvents: A comparative study. *Food Chemistry*, *342*, 128342.

Gottardo, S., Mech, A., Drbohlavová, J., Małyska, A., Bøwadt, S., Riego Sintes, J., & Rauscher, H. (2021). Towards safe and sustainable innovation in nanotechnology: State-of-play for smart nanomaterials. *NanoImpact*, *21*, 100297.

Hasheminya, S.-M., Rezaei Mokarram, R., Ghanbarzadeh, B., Hamishekar, H., & Kafil, H. S. (2018). Physicochemical, mechanical, optical, microstructural and antimicrobial properties of novel kefiran-carboxymethyl cellulose biocomposite films as influenced by copper oxide nanoparticles (CuONPs). *Food Packaging and Shelf Life, 17*, 196–204.

Heesterbeek, D., Martin, N., Velthuizen, A., Duijst, M., Ruyken, M., Wubbolts, R., Rooijakkers, S., & Bardoel, B. (2019). Complement-dependent outer membrane perturbation sensitizes gram-negative bacteria to gram-positive specific antibiotics. *Scientific Reports, 9*(1), 3074.

Hosseini, S. F., Rezaei, M., Zandi, M., & Ghavi, F. F. (2013). Preparation and functional properties of fish gelatin–chitosan blend edible films. *Food Chemistry*, *136*(3–4), 1490–1495.

Ili Balqis, A. M., Nor Khaizura, M. A. R., Russly, A. R., & Nur Hanani, Z. A. (2017). Effects of plasticizers on the physicochemical properties of kappa-carrageenan films extracted from Eucheuma cottonii. *International Journal of Biological Macromolecules, 103*, 721–732.

Jafarzadeh, S., & Jafari, S. M. (2020). Impact of metal nanoparticles on the mechanical, barrier, optical and thermal properties of biodegradable food packaging materials. *Critical Reviews in Food Science and Nutrition*, 1–19.

Jain, A., Kamble, R., & Patil, S. (2021). Electrospray technology as a probe for single step fabrication of glipizide loaded nanocochleates with enhanced bioavailability. *Journal of Dispersion Science and Technology*, 1–9.

Kamkar, A., Molaee-aghaee, E., Khanjari, A., Akhondzadeh-basti, A., Noudoost, B., Shariatifar, N., Alizadeh Sani, M., & Soleimani, M. (2021). Nanocomposite active packaging based on chitosan biopolymer loaded with nano-liposomal essential oil: Its characterizations and effects on microbial, and chemical properties of refrigerated chicken breast fillet. *International Journal of Food Microbiology*, *342*, 109071.

Khodayari, M., Basti, A. A., Khanjari, A., Misaghi, A., Kamkar, A., Shotorbani, P. M., & Hamedi, H. (2019). Effect of poly (lactic acid) films incorporated with different concentrations of Tanacetum balsamita essential oil, propolis ethanolic extract and cellulose nanocrystals on shelf life extension of vacuum-packed cooked sausages. *Food Packaging and Shelf Life, 19*, 200–209.

Klangmuang, P., & Sothornvit, R. (2016). Barrier properties, mechanical properties and antimicrobial activity of hydroxypropyl methylcellulose-based nanocomposite films incorporated with Thai essential oils. *Food Hydrocolloids, 61*, 609–616.

Kochańska, E., Łukasik, R. M., & Dzikuć, M. (2021). New circular challenges in the development of take-away food packaging in the COVID-19 period. *Energies, 14*(15), 4705.

Lopes, N. A., Pinilla, C. M. B., & Brandelli, A. (2019). Antimicrobial activity of lysozyme-nisin co-encapsulated in liposomes coated with polysaccharides. *Food Hydrocolloids, 93*, 1–9.

Malik, G. K., & Mitra, J. (2021). Zinc oxide nanoparticle synthesis, characterization, and their effect on mechanical, barrier, and optical properties of HPMC-based edible film. *Food and Bioprocess Technology, 14*(3), 441–456.

Marín-Silva, D. A., Rivero, S., & Pinotti, A. (2019). Chitosan-based nanocomposite matrices: Development and characterization. *International Journal of Biological Macromolecules, 123*, 189–200.

Mihalca, V., Kerezsi, A. D., Weber, A., Gruber-Traub, C., Schmucker, J., Vodnar, D. C., Dulf, F. V., Socaci, S. A., Fărcaș, A., & Mureșan, C. I. (2021). Protein-based films and coatings for food industry applications. *Polymers, 13*(5), 769.

Mohamed, S. A., El-Sakhawy, M., & El-Sakhawy, M. A. –M. (2020) Polysaccharides, protein and lipid-based natural edible films in food packaging: A review. *Carbohydrate Polymers*, *238*, 116178.

Motelica, L., Ficai, D., Ficai, A., Oprea, O. C., Kaya, D. A., & Andronescu, E. (2020). Biodegradable antimicrobial food packaging: Trends and perspectives. *Foods, 9*(10), 1438.

Motta, J. F. G., de Souza, A. R., Gonçalves, S. M., Madella, D. K. S. F., de Carvalho, C. W. P., Vitorazi, L., & de Melo, N. R. (2020). Development of active films based on modified starches incorporating the antimicrobial agent lauroyl arginate (LAE) for the food industry. *Food and Bioprocess Technology, 13*(12), 2082–2093.

Nazir, S., & Azad, Z. A. A. (2019). Food nanotechnology: An emerging technology in food processing and preservation. In A. Malik, Z. Erginkaya, & H. Erten (Eds.), *Health and Safety Aspects of Food Processing Technologies* (pp. 567–576). Cham: Springer.

Niaz, T., Shabbir, S., Noor, T., & Imran, M. (2019). Antimicrobial and antibiofilm potential of bacteriocin loaded nano-vesicles functionalized with rhamnolipids against foodborne pathogens. *LWT*, *116*, 108583.

Niaz, T., Shabbir, S., Noor, T., Abbasi, R., Raza, Z. A., & Imran, M. (2018). Polyelectrolyte multicomponent colloidosomes loaded with nisin Z for enhanced antimicrobial activity against foodborne resistant pathogens. *Frontiers in Microbiology*, *8*, 2700.

Ortiz-Duarte, G., Martínez-Hernández, G. B., Casillas-Peñuelas, R., & Pérez-Cabrera, L. E. (2021). Evaluation of biopolymer films containing silver–chitosan nanocomposites. *Food and Bioprocess Technology, 14*(3), 492–504.

Paula, G. A., Benevides, N. M. B., Cunha, A. P., de Oliveira, A. V., Pinto, A. M. B., Morais, J. P. S., & Azeredo, H. M. C. (2015). Development and characterization of edible films from mixtures of κ-carrageenan, ι-carrageenan, and alginate. *Food Hydrocolloids, 47*, 140–145.

Pérez, P. F., Ollé Resa, C. P., Gerschenson, L. N., & Jagus, R. J. (2021). Addition of zein for the improvement of physicochemical properties of antimicrobial tapioca starch edible film. *Food and Bioprocess Technology, 14*(2), 262–271.

Polat, T. G., Duman, O., & Tunc, S. (2020). Preparation and characterization of environmentally friendly agar/κ-carrageenan/montmorillonite nanocomposite hydrogels. *Colloids and Surfaces A: Physicochemical and Engineering Aspects*, *602*, 124987.

Priyadarshi, R., & Negi, Y. S. (2017). Effect of varying filler concentration on zinc oxide nanoparticle embedded chitosan films as potential food packaging material. *Journal of Polymers and the Environment, 25*(4), 1087–1098.

Rehman, A., Jafari, S. M., Aadil, R. M., Assadpour, E., Randhawa, M. A., & Mahmood, S. (2020). Development of active food packaging via incorporation of biopolymeric nanocarriers containing essential oils. *Trends in Food Science & Technology, 101*, 106–121.

Sahraee, S., Ghanbarzadeh, B., Milani, J. M., & Hamishehkar, H. (2017). Development of gelatin bionanocomposite films containing chitin and ZnO nanoparticles. *Food and Bioprocess Technology, 10*(8), 1441–1453.

Samsalee, N., & Sothornvit, R. (2020). Characterization of food application and quality of porcine plasma protein–based films incorporated with chitosan or encapsulated turmeric oil. *Food and Bioprocess Technology, 13*(3), 488–500.

Santos, J. C., Sousa, R. C., Otoni, C. G., Moraes, A. R., Souza, V. G., Medeiros, E. A., ... & Soares, N. F. (2018). Nisin and other antimicrobial peptides: Production, mechanisms of action, and application in active food packaging. *Innovative Food Science & Emerging Technologies*, *48*, 179–194.

Sedayu, B. B., Cran, M. J., & Bigger, S. W. (2020). Improving the moisture barrier and mechanical properties of semi-refined carrageenan films. *Journal of Applied Polymer Science, 137*(41), 49238.

Seyedabadi, M. M., Rostami, H., Jafari, S. M., & Fathi, M. (2021). Development and characterization of chitosan-coated nanoliposomes for encapsulation of caffeine. *Food Bioscience*, *40*, 100857.

Shiroodi, S. G., Nesaei, S., Ovissipour, M., Al-Qadiri, H. M., Rasco, B., & Sablani, S. (2016). Biodegradable polymeric films incorporated with nisin: Characterization and efficiency against listeria monocytogenes. *Food and Bioprocess Technology, 9*(6), 958–969.

Souza, M. P., Vaz, A. F. M., Costa, T. B., Cerqueira, M. A., De Castro, C. M. M. B., Vicente, A. A., & Carneiro-da-Cunha, M. G. (2018). Construction of a biocompatible and antioxidant multilayer coating by layer-by-layer assembly of κ-carrageenan and quercetin nanoparticles. *Food and Bioprocess Technology, 11*(5), 1050–1060.

Sun, G., Chi, W., Zhang, C., Xu, S., Li, J., & Wang, L. (2019). Developing a green film with pH-sensitivity and antioxidant activity based on κ-carrageenan and hydroxypropyl methylcellulose incorporating Prunus maackii juice. *Food Hydrocolloids, 94*, 345–353.

Swaroop, C., & Shukla, M. (2019). Development of blown polylactic acid-MgO nanocomposite films for food packaging. *Composites Part A: Applied Science and Manufacturing*, *124*, 105482.

Tan, C., Wang, J., & Sun, B. (2021). Biopolymer-liposome hybrid systems for controlled delivery of bioactive compounds: Recent advances. *Biotechnology Advances*, *48*, 107727.

Tibolla, H., Pelissari, F. M., Martins, J. T., Lanzoni, E. M., Vicente, A. A., Menegalli, F. C., & Cunha, R. L. (2019). Banana starch nanocomposite with cellulose nanofibers isolated from banana peel by enzymatic treatment: In vitro cytotoxicity assessment. *Carbohydrate Polymers, 207*, 169–179.

Wrona, M., Cran, M. J., Nerín, C., & Bigger, S. W. (2017). Development and characterisation of HPMC films containing PLA nanoparticles loaded with green tea extract for food packaging applications. *Carbohydrate Polymers, 156*, 108–117.

Zhong, H., Gao, X., Cheng, C., Liu, C., Wang, Q., & Han, X. (2020). The structural characteristics of seaweed polysaccharides and their application in gel drug delivery systems. *Marine Drugs, 18*(12), 658.

Zhu, M., Ge, L., Lyu, Y., Zi, Y., Li, X., Li, D., & Mu, C. (2017). Preparation, characterization and antibacterial activity of oxidized κ-carrageenan. *Carbohydrate Polymers., 174*, 1051–1058.